RESEARCH ARTICLE

*European Journal of Environment and Earth Sciences*
*www.ej-geo.org*

# Inventory of Ring Structures in N- and W-Morocco based on Satellite Data

Barbara Theilen-Willige

**ABSTRACT**

**This study is focused on the detection of circular features with different sizes, origins, and state of erosion as well as on their surrounding tectonic pattern based on satellite images of North- and West- Morocco. Sentinel 2- and Landsat 8/9-images and Sentinel 1 radar data help to identify larger ring structures and smaller circular features. Digital Elevation Model (DEM) data and the DEM derived morphometric maps support these investigations in a GeoInformation System (GIS) embedded environment. The evaluations of the various satellite data, especially after digital image processing of the thermal bands, contribute to the inventory larger ring structures with diameters of 10 km up to more than 50 km related to magmatic intrusions or to salt domes in the subsurface with varying grades of erosion. Some of these larger ring structures are only visible on morphometric maps, traced by circular arrangements of slope gradients or a concentric drainage pattern. Smaller circular features such as volcanic features (cinder cones, calderas, maars), and sinkholes in karst environments with diameters ranging from several 10 m up to more than 500 m were digitized as well. As karst phenomena, volcanic features or halotectonic movements may cause damage to the infrastructure the inventory of ring structures should be part of a natural hazard GIS.**

**Keywords:** Circular Structures, GIS, Morocco, Remote Sensing.

**Published Online:** January 24, 2023

**ISSN**: 2684-446X

**DOI**: 10.24018/ejgeo.2023.4.1.364

**B. Theilen-Willige ***
Technische Universität Berlin (TUB),
Faculty VI, Berlin, Germany
(e-mail:
barbara.theilen-willige@campus.tu-berlin.de)

**Corresponding Author*

## I. Introduction

Although a large amount of research has been carried out related to the geologic history and structural and tectonic inventory in Northern Morocco [1]-[3] combined evaluations of different satellite data can contribute to furtheradditional knowledge. After previous evaluations of optical and radar satellite images and digital elevation data from northern Morocco [4] it became obvious, that there are somecircular structures visible on the satellite images and onmorphometric maps that were neither documented on available geologic maps, nor described in the geologic literature. The reasons for this vary according to the specific situation. Some circular structures are buried underneath younger lithologic units and not visible in the field, but still on satellite data because of the concentric arrangement of thedrainage pattern or vegetation anomalies.

The combination of different remote sensing data is used in the scope of this study to derive an overview of structural information in N-and W-Morocco and focus on an inventory of circular features of different sizes and origins and their surrounding tectonic pattern. Fig. 1 provides an overview of the visible circular features on the satellite images.

Crystalline rocks were formed mainly in the deeper part of the earth, at a depth of several tens of kilometers. When formed as plutons and then brought to the surface during the erosion of the strata above, they are often visible as ring structures.

Smaller circular features situated in areas covered by forests are very difficult to detect, partly not even on radar images. Thus, the results cannot be not complete based on remote sensing alone. Field work and a careful further analysis of references is required to avoid errors.

As some of the circular features are not indicated on geologic maps and, thus, seem to be unknown so far, this study aims to contribute to the systematic detection and inventory of ring structures.

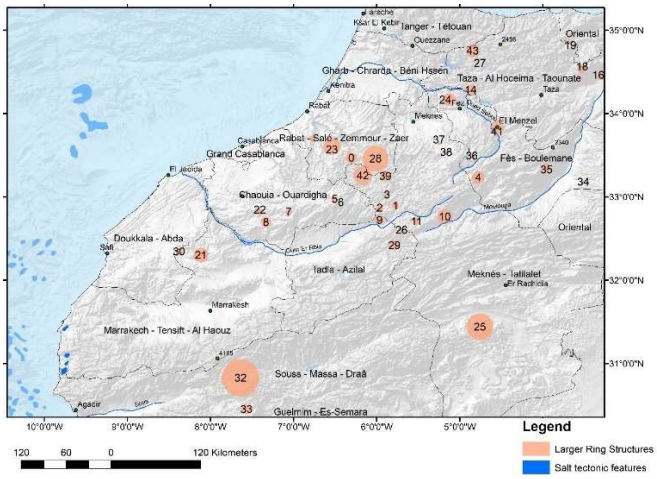


Fig. 1. Structural traces of ring structures derived from satellite data in N- and NW-Morocco. The numbers are related to the position of the case examples presented in this study.

*European Journal of Environment and Earth Sciences*
*www.ej-geo.org*

In the scope of this inventory structural details related to the tectonic pattern around the ring structures could be added. Fig. 2 provides an example of available geologic information of the areas where circular features were derived from satellite data.

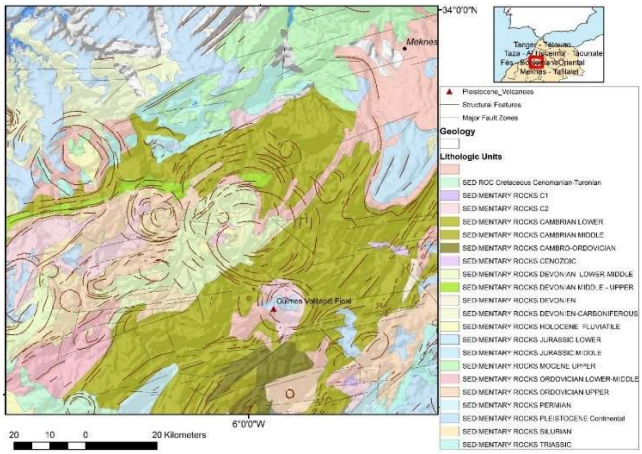


Fig. 2. Geologic map and the outline of ring structures derived from the evaluation of satellite images (geologic shapefiles: Geologic Overview derived from data from the British Geological Survey provided by the US Geological Survey [7], and the OneGeology-Portal [8], and [9], structural features, major lineaments: derived from evaluations of satellite data). Most of the larger ring structures occur in the Cambro-Ordovician-Silurian lithologic units.

An inventory of circular structures is important for several reasons such as for hydrogeologic investigations because the groundwater flow is influenced by those structures due to varying permeabilities within fault and fracture zones. Concentric and radial faults and dislocations might form a hindrance for the groundwater flow and/or lead to the development of springs, depending on the specific situation. Within larger, brittle fault zones the water flow can augment. A detailed structural analysis is of interest as well or for the mining industry. Ore deposits have often occurred within circular structures related to magmatic intrusions.

Another reason for the detailed inventory of circular structures is the monitoring of potential geohazards. The larger ring structures seem to have an influence on earthquake activity. When analyzing the earthquake density of earthquakes during the last decades, it seems obvious that the earthquake density is lower in areas with larger ring structures (EMSC, USGS, ISC-data base) [5]-[7] and higher in the folded Middle Atlas with larger extended fault zones. Fig. 3 shows the earthquake density in the Middle Atlas area combined with the detected circular structural features.

Another example for the importance of geohazard monitoring is the collapse of sinkholes affecting the safety of infrastructure.

The different forms of volcanic activity might be a risk for the land use. Halotectonic movements and salt strata activity buried beneath a sedimentary stratum might cause problems aswell for the infrastructure.

The following main circular features can be distinguished:

a) A large circular structure with more than 100 km in diameter in the Rif area and around the Alboran Sea.
b) Larger circular structures of more than 10 km in diameter, obviously domes related to magmatic intrusions into the subsurface and up to the surface.
c) Larger ring structures near the coast related to halotectonic features such as salt domes.
d) Smaller circular volcanic features such as cinder cones, calderas, ranging from 10 m up to 2 km in diameter.
e) Sinkholes in varying diameters in karst environments.
f) Deflation hollows due to wind erosion.
g) Traces of gas release and seeps within smaller, circular structures.
h) Impact craters.

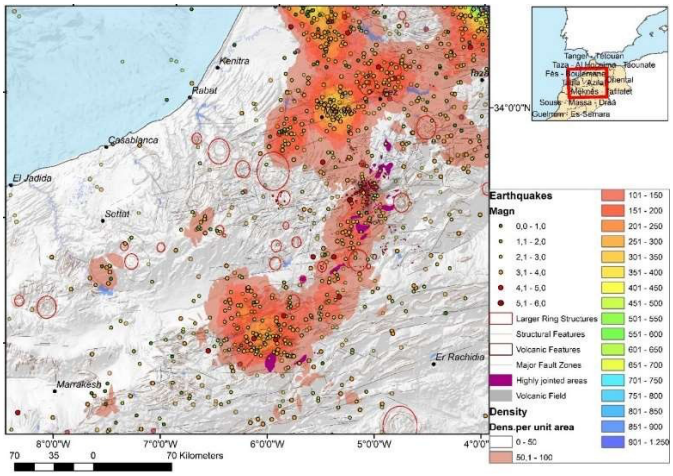


Fig. 3. Earthquake density in the Middle Atlas and Anti-Atlas (data of epicenters from EMSC, USGS and ISC [5]-[7]. and occurrence of larger ring structures.

## II. Geographic Overview

The Middle Atlas Mountain range can bedivided into two geomorphological provinces:1) an elevated, flat area called Tabular Middle Atlas, which is located in the north-western orogenic sectors and consists of weakly deformed Mesozoic sediments in stratigraphic contact with the Paleozoic basement of the western Meseta, and 2) the deeply dissected, high-relief Folded Middle Atlas. Fig. 4 shows the height levels in NW-Morocco and provides an overview of the complex geomorphologic setting in the investigation area, ranging of flat lowlands, basins, and mesetas to elongated mountainous areas. Most of the larger ring structures are situated within height levels between 600-1000 m. Seismicity and geomorphic landforms suggest that tectonic deformation is still active, at least in some sectors of the orogen [10], [11].

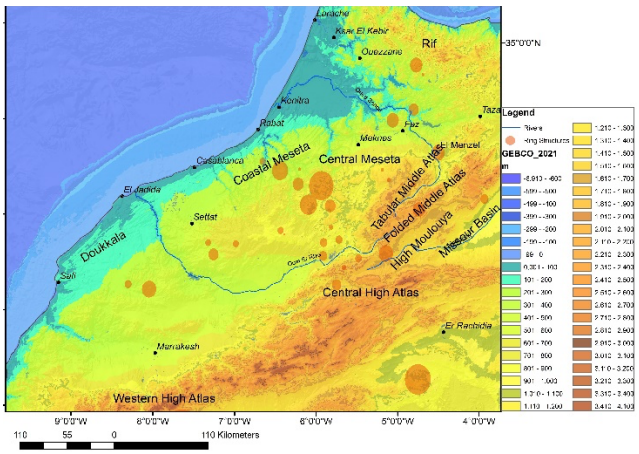


Fig. 4. Height level map based on GEBCO data. Most of the larger circular features are situated in height levels between 500-1000 m.

*European Journal of Environment and Earth Sciences*
*www.ej-geo.org*

## III. Geologic Overview

Morocco is located northwest of the mainland of the African plate. This part of the plate is characterized by a long evolution from the Proterozoic to the present time [12]. The consequences have been the installation during the Proterozoic of agglomerated Cratonic blocks, a peneplanation starting at the beginning of the Phanerozoic [13], the Cenozoic convergence of Africa-Europe, in the context of the evolutions of the Atlantic ridge and the Atlasic rift.

All along the intense tectonic and geological evolution, several episodes of orogenesis took place [13]. During superimposed orogenic cycles, continental deformation concentrated in large-scale fault networks and structures that are frequently reactivated over long time scales [14].

Morocco exhibits a wide variety of magmatic events from Archean to Quaternary being the cause of most of the larger ring structures visible on the satellite images and maps derived from satellite data.

Mesoproterozoic magmatism is represented by a small number of mafic dykes [15]. Massive Neoproterozoic magmatic activity, related to the Pan-African cycle, consists of rift-related magmatism associated with the Rodinia breakup, an Early Cryogenian convergent margin event (760–700 Ma), syn-collisional magmatism (680–640 Ma), followed by widespread magmatism (620–555 Ma). Each magmatic episode corresponded to a different geodynamic environment and produced different types of magma [16].

Phanerozoic magmatism began with Early Cambrian basaltic volcanism, which persisted during the Middle Cambrian, and into the Early Ordovician. Late Devonian and Carboniferous, pre-Variscan tholeiitic and calc-alkaline (Central Morocco) volcanic flows in basins of the Moroccan Meseta. The Late Carboniferous Variscan event was accompanied by the emplacement of 330–300 Ma calc-alkaline granitoids in upper crustal shear zones. Post-Variscan alkaline magmatism was associated with the opening of the Permian basins.

Mesozoic magmatism began with the huge volumes of magma emplaced around 200 Ma in the. Central Atlantic Magmatic Province (CAMP). This volcanism occurs in all structural domains of Morocco, from the Anti-Atlas to the External Rif domain with a peak activity around 199 Ma. A second Mesozoic magmatic event is represented by mafic lava flows and gabbroic intrusions in the Internal Maghrebian flysch nappes as well as in the external Meso-Rif. The Central High Atlas also records Early Cretaceous alpine Tethys magmatism associated with the aborted Atlas rift, or perhaps linked to plume activity [16].

Cenozoic magmatism is associated with Tertiary and Quaternary circum-Mediterranean alkaline provinces and is characterized by an intermittent activity over 50 Ma from the Anti-Atlas to the Rif [17].

Another cause for the development of larger circular and elongated structures is related to halokinesis in the coastal areas of NW- and W-Morocco. The salt basins of Morocco and Mauritania were developed on the NW African margin of the Central Atlantic. The age of the salt layers in Morocco is dated Upper Triassic to Liassic, as Central Atlantic Magmatic Province basalts can be found within it [18], [19]. The Moroccan salt basin on average is ~50-150 km in width, but it stretches for at least 1000 km between the leading edge of the offshore pre-Rifean nappe in the north and the Canary Islands in the south. The significant along-strike variations in the cross-sectional and map-view distribution of the Upper Triassic to Lower Jurassic salt reflect its uneven original distribution. The seismically mapped individual salt structures such as tongues, sheets, and canopies might have originated from an autochthonous salt layer deposited in somewhat isolated half-grabens.

Fig. 5 provides an overview of the lithologic units in North-Morocco.

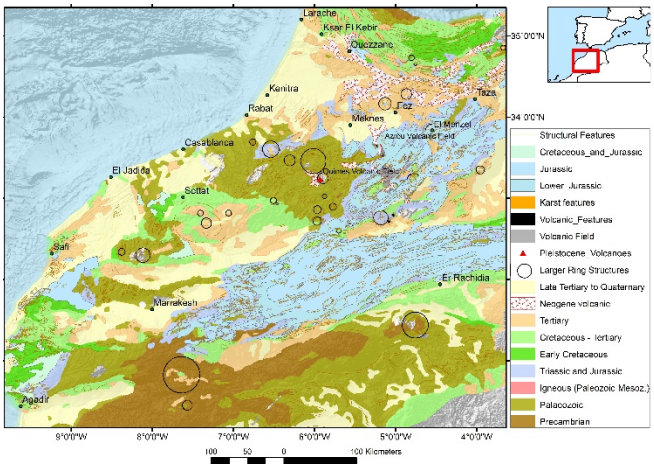


Fig. 5. Geologic overview [8], [9], [20], [21].

## IV. Methods

When analyzing the geological, geophysical, and satellite data traces of structures such as faults, folding and domes are often clearly visible on satellite imageries, because morphologic surface changes related to tectonic structures are traced on height level or slope gradient maps derived from DEM data.

Thus, the interdisciplinary approach used in the scope of this research comprises evaluations of remote sensing data, geological, geophysical, and topographic data, integrated into a GIS environment. Earthquake data were provided by the European-Mediterranean Seismological Centre (EMSC), International Seismological Centre (ISC), and US Geological Survey (USGS). Satellite imageries and Digital Elevation Model (DEM) data [22] were used then for generating a GIS data base and combined with different geodata and available geologic maps. Satellite data were processed and evaluated such as Sentinel 1 – C-Band, Synthetic Aperture Radar (SAR) data and optical Sentinel 2 images [23], and Landsat optical data (Landsat TM and Landsat 8 and 9 of the Operational Land Imager-OLI) [22].

Infrastructural shapefiles from Morocco were downloaded from the Geofabrik's download server [24]. The shapefiles related to ring structures, lineaments, structural features, karst phenomena and volcanic features were digitized based on the different satellite images. Especially Sentinel 1 radar images reveal larger fault zones, for example by dislocations of lithologic units.

### *A. Digital Image Processing of Different Optical and Radar Satellite Data*

ENVI software from Harris Geospatial Solutions and the Sentinel Application Platform (SNAP) provided by ESA [23]

were used for the digital image processing of the optical Landsat, Sentinel 2 and ASTER data. SNAP from ESA provided the tools as well for the processing of radar data. The evaluation of Sentinel 1 A and B radar images requires geometric correction and calibration. Digital image processing of LANDSAT 5 Thematic Mapper and Landsat 8/9 - The Operational Land Imager (OLI) data was carried out by merging different Red Green Blue (RGB) band combinations with the panchromatic Band 8 to pan-sharpen the images. Based on Sentinel 2 data water index (Normalized Difference Water Index -NDWI) image products were derived.

### *B. Evaluations of DEM Data*

Digital Elevation Model (DEM) data from the Shuttle Radar Topography Mission (SRTM), and ASTER DEM data (both with about 30 m spatial resolution) are covering the whole investigation area. The Advanced Land Observing Satellite-1 (ALOS), Phased Array type L-band Synthetic Aperture Radar (PALSAR) from the Japan Aerospace Exploration Agency (JAXA) provided data with 12,5 m spatial resolution, however, not a complete coverage. The satellite data were downloaded from open sources such as USGS / Earth Explorer, Sentinel Hub / ESA, Alaska Satellite Facility (ASF) [25]. Another set of DEM data was provided by the German Aerospace Center (DLR) delivering TerraSAR-X-DEM data (resolution of 90 m) [26]. The data were processed using geoinformation systems ArcGIS from ESRI and QGIS, a free and Open Source Geographic Information System. Mosaics were created based on the various DEM data.

## V. Inventory of Ring Structures based on SatelliteData

In the following chapters an overview of different circular structures and their expressions on satellite images and morphometric maps is presented. In most cases their origin can be derived, however, in some cases clarifying their origin remains for future investigations.

In the scope of this study evaluations of morphometric maps play an important role because ring structures sometimes can be traced more clearly on slope gradient, height level or drop raster maps than on other satellite images. Optical, digital processed and enhanced satellite images are then correlated with the morphometric maps. Especially, when combing the thermal bands of optical satellite data in an RGB image structural features are enhanced due to brightness differences. The visibility of ring structures on radar images depends on the radar-illumination geometry and the surface roughness. Larger circular structures appear on the different morphometric maps and satellite images.

### *A. Larger Ring Structures*

The most prominent and largest circular structure becomes visible on Landsat (Fig. 6), GEBCO bathymetric data (Fig. 7) and SRTM DEM data covering the Alboran Sea [27]. The Betic-Rif Orogen surrounding the Alboran Sea consists of arcuate mountain belts with a northern branch formed by the Betic cordillera in the Iberian Peninsula and a southern branch formed by the Rif chain in northern Africa. These arcuated mountain belts as a whole form a large ring structure (Fig. 6 and Fig. 7). The Betic-Rif orogenic belts are situated between two colliding continents: between the African and Eurasian plates. Present-day tectonic processes occur within the context of ongoing convergence between Africa and Iberia.

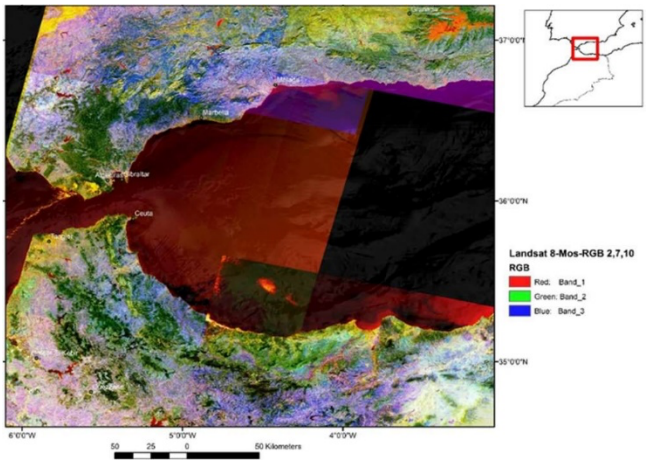


Fig. 6. Landsat 5-mosaic of images acquired between 1972 and 1975 of the Alboran ring structure.

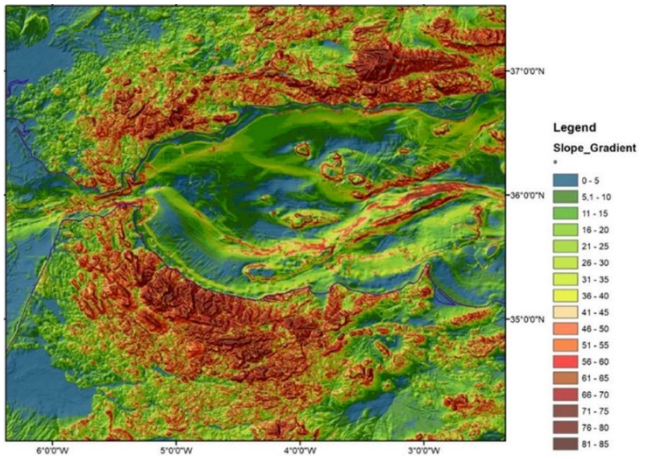


Fig. 7. Slope gradient map of the Alboran Sea and adjacent areas derived from GEBCO 2021 data [27].

The question arises whether an additional hypothesis about the origin of this circular structure by an asteroid impact might be discussed because of its similarity with large, known cosmic impact craters.

The next large ring structure is situated between 6°10′W and 5°40′ W longitude, 33°20′ N and 33°40’ N latitude. Fig. 8a shows the Landsat 8-scene (RGB combining thermal bands7 and 10 with band 2) of this ring structure with a diameter of about 30-40 km with a flat basin at the center. The available geologic data indicate Paleozoic rocks, mainly Silurian sedimentary outcrops. Granites of about 300 MA embedded in Silurian series form the center of this structure [21]. Granite plutons doming up the strata above might be the reason for the circular structures in this area.

Fig. 8b presents the derived Principal Component image product of the same area and Fig. 8c the Sentinel 2-scene. This circular outline is not indicated in the available geologic maps and shapefiles [9]. However, the circular arrangement of structural traces is clearly visible. The morphometric maps derived from ALOS PALSAR DEM data with 12,5 m spatial resolution reveal details of traces of circular structures (Fig. 9a and 9b), especially by the evaluation of the slope gradient map.

*European Journal of Environment and Earth Sciences*
*www.ej-geo.org*

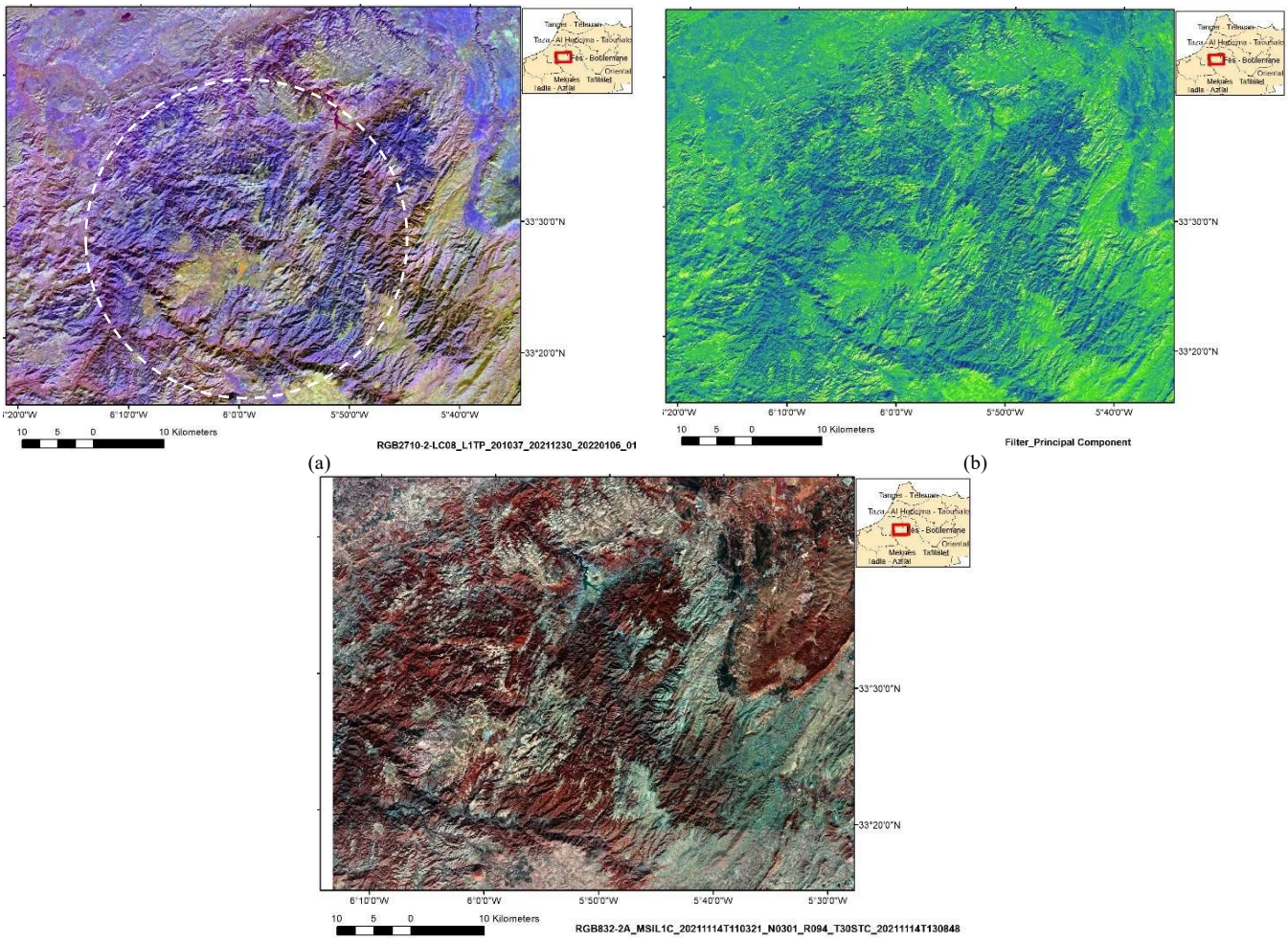


(a) (b) (c)

Fig. 8. a) Large circular structure visible on a Landsat 8-sene combining thermal bands 7 and 10 (Number 28 on Fig. 1); b) Principal component of the image data; c) Sentinel 2 scene of the same area.

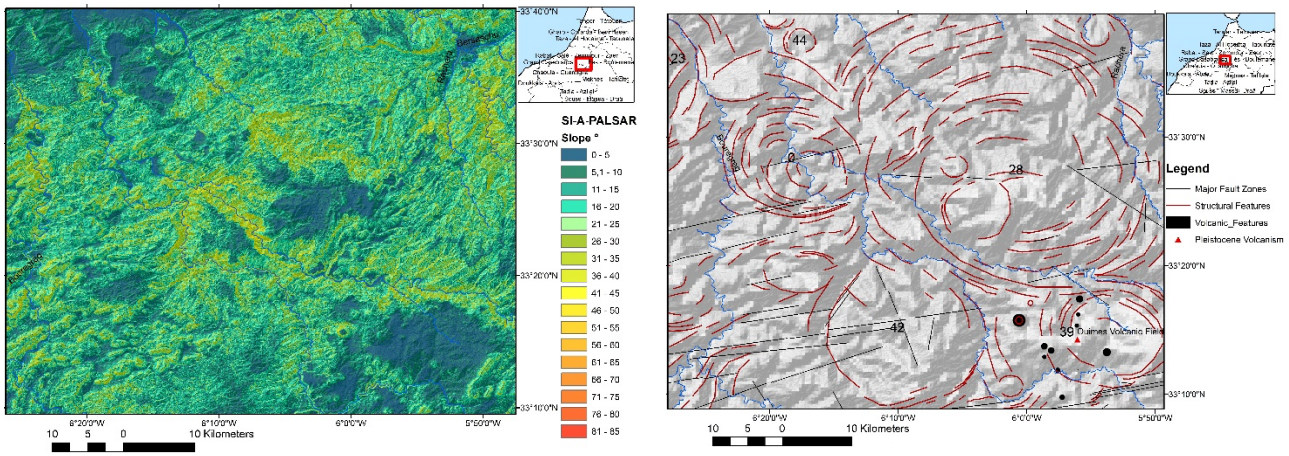


(a) (b)

Fig. 9. a) Slope gradient map derived from ALOS PALSAR DEM data; b) Structural evaluation of the slope gradient map.

The following ring structure (number 0 on Fig. 9b) became visible because of the evaluations of this slope gradient map based on ALOS-PALSAR-DEM data (Fig. 10a). On available geologic maps there is no evidence of its existence [21]. The Landsat 8 scene (Fig. 10b) helps to identify this structure.

The next example shows a ring structure on the satellite scenes situated between 6°40′W and 6°50′W and 33°39′N and 33°44′N within sedimentary Devonian- Carboniferous rocks with a diameter of about 8 km (Fig. 11a, 11b, and 11c).

The inner ring, bordered by the Qued Grou-river along its eastern part, is clearly circular, whereas the outer ring appears more oval-shaped, elongated in W-E direction. Due to the subtle radar reflection of the terrain on the radar image the ring structure is visible as well (Fig. 11b). The slope gradient map (Fig. 11c) clearly outlines theconcentric arrangement of valleys and hills.

*European Journal of Environment and Earth Sciences*
*www.ej-geo.org*

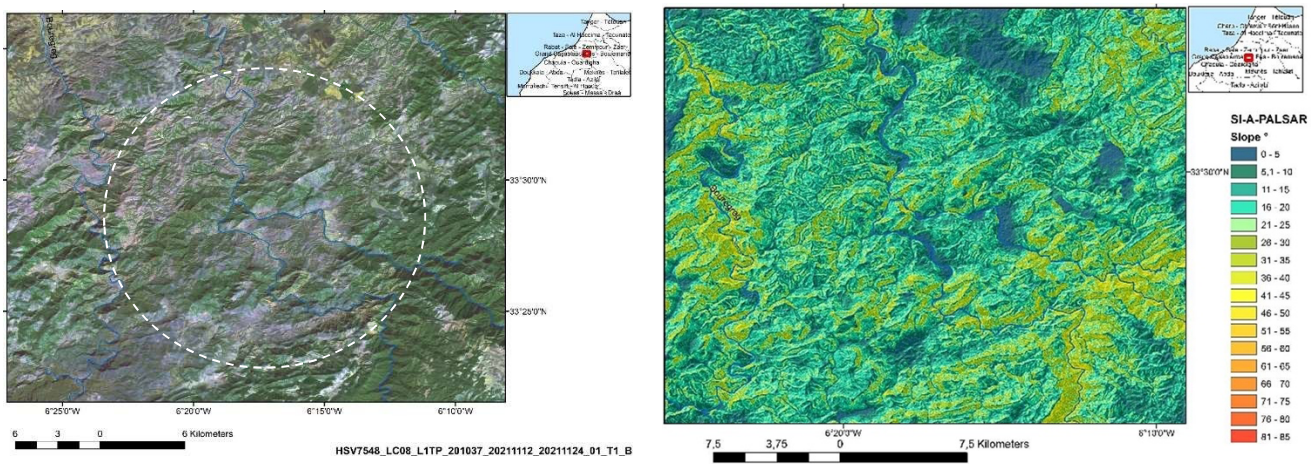


(a) (b)

Fig. 10. a) Circular structure (0 on Fig.1) visible on a slope gradient map; b) Landsat 8-scene of the same areas as (a).

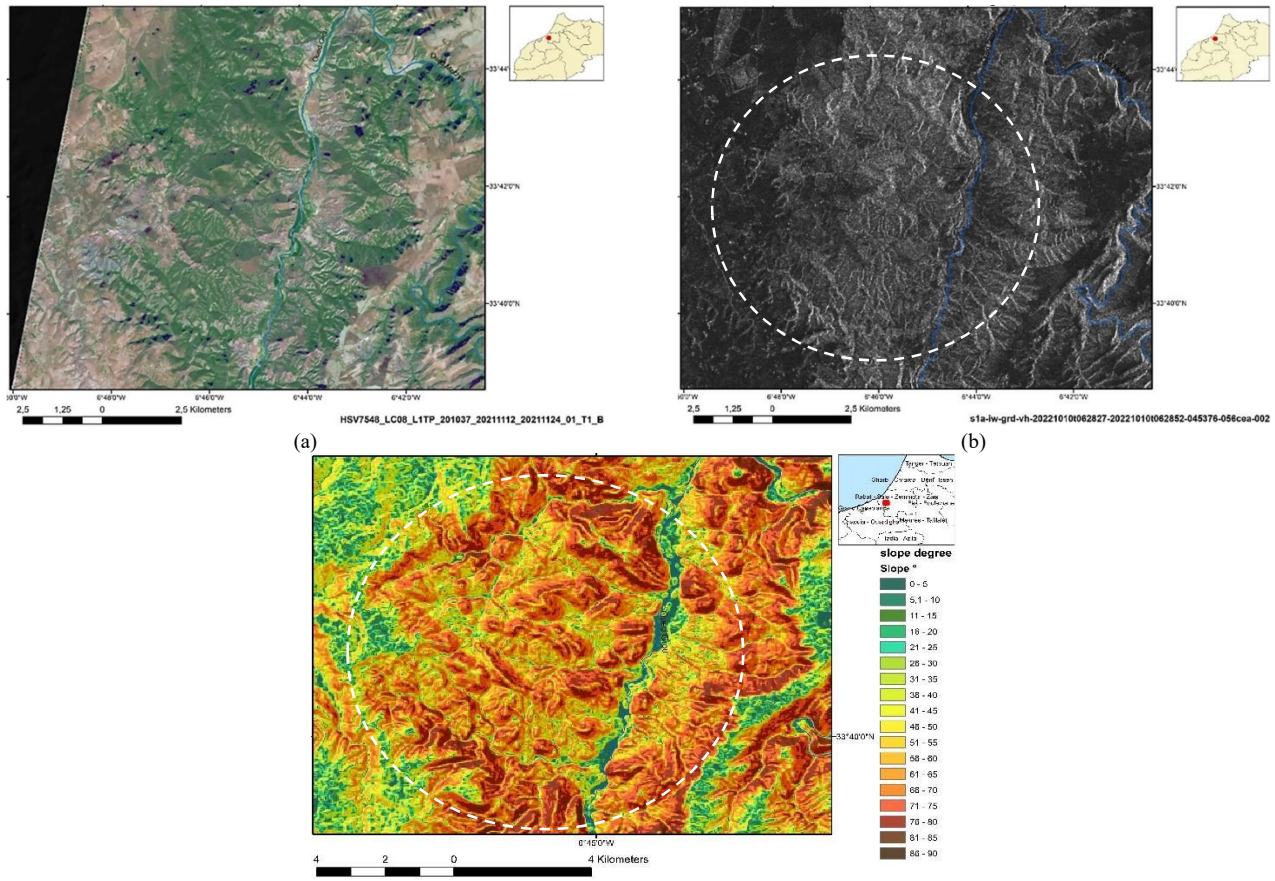


(a) (b)

(c)

Fig. 11. a) Ring structure visible on a Landsat 8-scene (Number 40 on Fig. 1); b) Sentinel 1-radar scene.
c) Slope gradient map derived from SRTM-DEM-data.

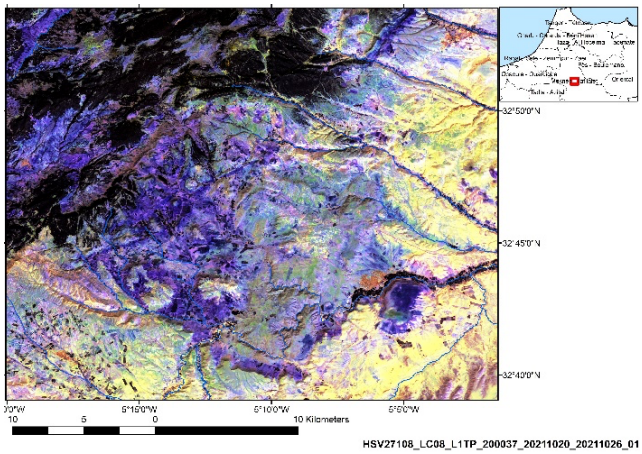


Fig. 12. Landsat 8 RGB image of bands 2,7 and 10 revealing a circular structure (number 10 on Fig. 1).

Fig. 12 shows a large circular shaped structure of about 20 km in diameter within 5°20′W and 5°50′W longitude and 32°40′N and 32°50’N latitude. Triassic, Jurassic, and Cretaceous sedimentary outcrops can be derived from the geologic shapefiles. Volcanic rocks are visible at the southeastern border.

The next ring structure is related to Carboniferous granites (about 300 MA) according to the geologic map (1 : 1 Mio) [21]. The circular outline visible on the satellite images (Fig. 13) is not indicated on the geologic map and within the lithologic shapefile data. Based on the same Sentinel 2 data as in Fig. 13a, the water-index was calculated using Bands 3 and 12. The color-coded result is shown in Fig. 13b, the radar scene in Fig. 13c. Thus, the evaluation of the satellite images provides additional structural information.

The more oval-shaped structure in Fig 14 is related to Carboniferous granites (about 300 MA) according to the geologic map (1: 1 Mio) [21]. This granite complex is situated between 8°00W to 8°15’W and 32°10 N to 32°25’N. It is traced on the slope gradient map (Fig. 14a) and on the radar satellite image (Fig. 14b). The evaluation of the satellite data allows a more precise delineation of the whole structure.

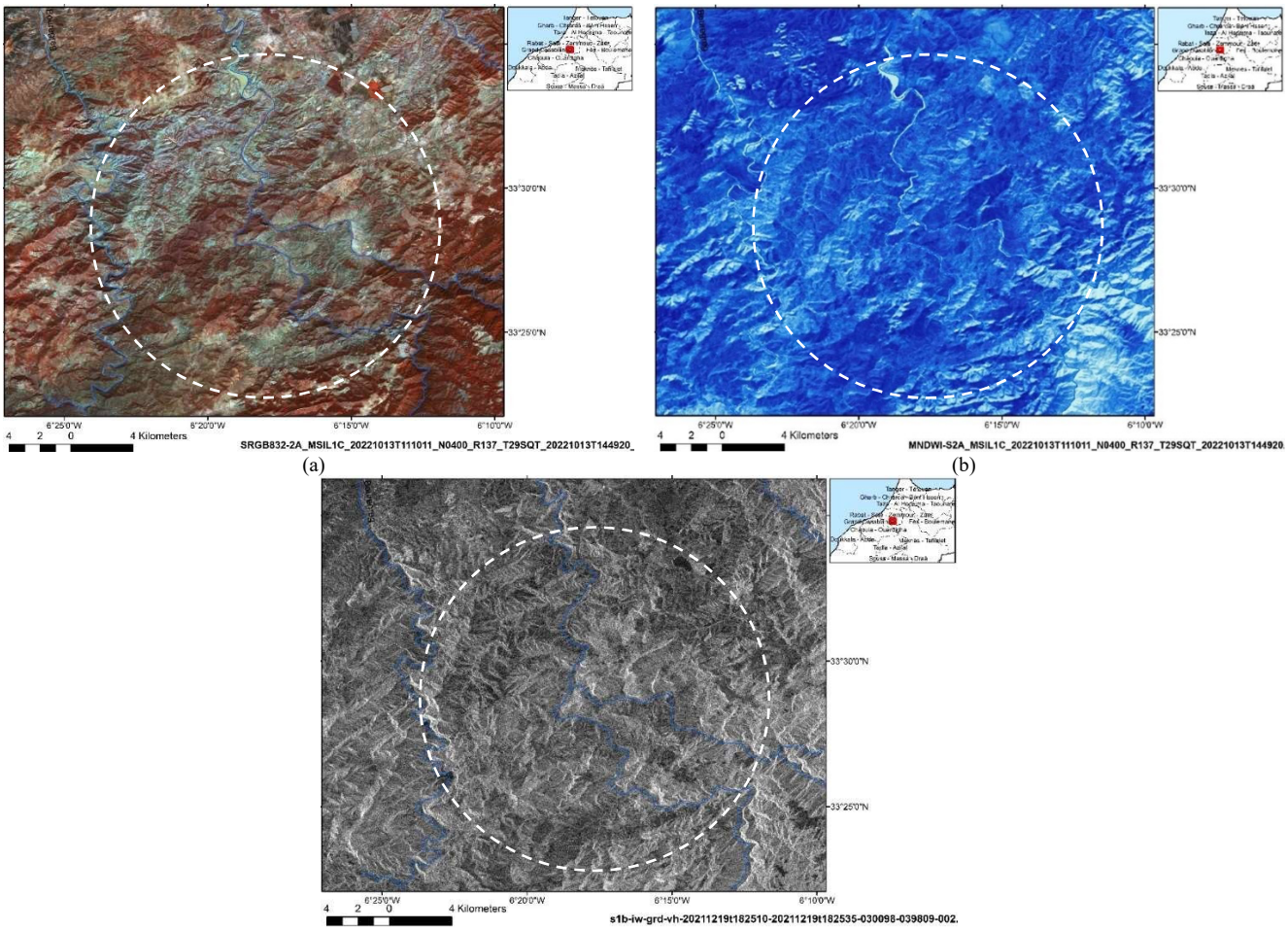


Fig. 13. a) Sentinel 2- RGB (Bands 8,4 and 2) from the ring structure. Granite outcrops were documented at the center; b) Sentinel 2-color-coded water index scene of the ring structure; c) Sentinel 1 radar scene of the ring structure enhancing the circular outline.

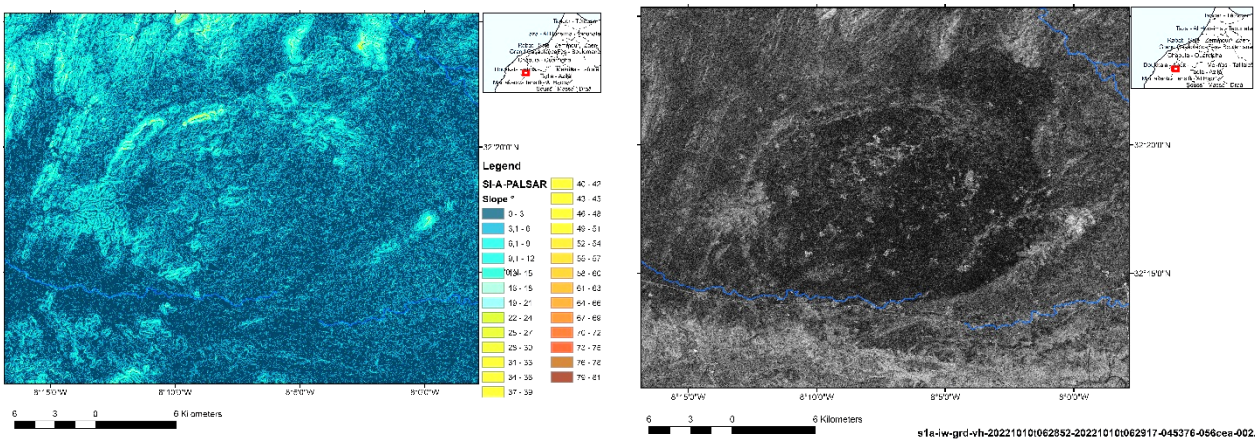


Fig. 14. a) Slope gradient map of the granite complex; b) Sentinel 1-radar scene of the granite complex.

Fig. 15 reveals a circular structure on a Landsat scene (4°50′W to 4°56′W, 33°26′N to 33°33′N). There was no information available about this circular structure.

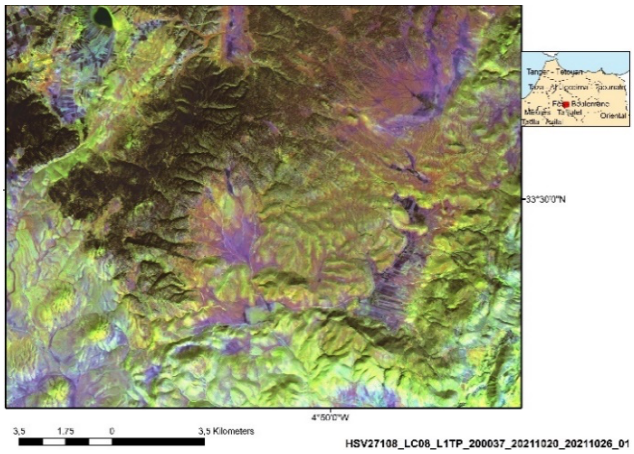


Fig. 15. Unknown ring structure. Along the eastern part of this ring structure, enough groundwater is available for agriculture in this arid environment.

Whereas the previous examples are more related to magmatism, the next examples of large structures are caused by halotectonic movements, especially by salt diapirism along the coast. The seismically mapped individual salt structures such as tongues, diapirs, sheets, and canopies might have originated from autochthonous salt layers [10], [18], [19].

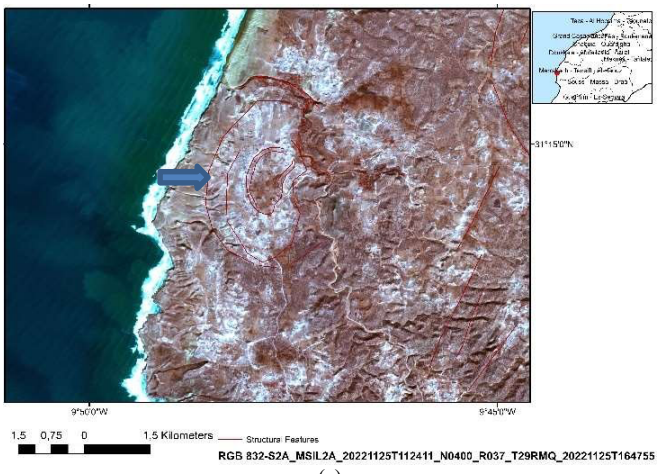


(a)

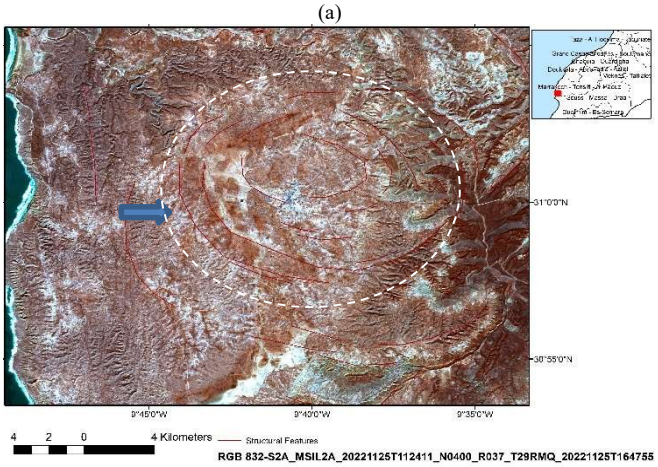


(b)

Fig. 16. a) Salt tectonic features at the Atlantic west coast visible on Sentinel 2-scenes; b) Large circular structure within Jurassic and Cretaceous strata.

Structures have formed during continued sedimentary loading due to gravitational instability and tectonic activity. By up-doming the strata above some of the surface-near salt structures are visible on satellite images as circular and oval structures (Fig. 16a and 16b) in the coastal areas of W-Morocco, especially near the city of Essaouira. The oval-shaped structures in the next figures become visible due to differences in the soil moisture causing tonal variations on the Sentinel 2-scenes.

### *B. Smaller Ring Structures*

Smaller circular features such as volcanic features (cinder cones, calderas, maars), and sinkholes in karst environments with diameters ranging from several 10 m up to more than 500 m were mapped as well as far as possible based on remote sensing data. Through the tabular morphology of the northwestern part of the Middle Atlas in Morocco, numerous volcanoes arise together with pyroclastic product layers and lava flows, the majority of which are Strombolian cinder cones, and some correspond to maars relayed by strombolian activity [28], [29]. The volcanic shape spectrum, such as cones, maars, tuff-rings, and cone-maar mixes, generally is associated with a later lava flow discharge that could develop many surfaces and appearances. There are eruptive products such as pahoehoe lava, scoria, tuff, lapilli, base-surges, bombs, etc. [30], [31]. The complex interference of the different geologic settings influencing the development of circular features such asvolcanic intrusions into limestones leading to circular features with complex origin requires intense field work to verify the situation (Fig. 17).

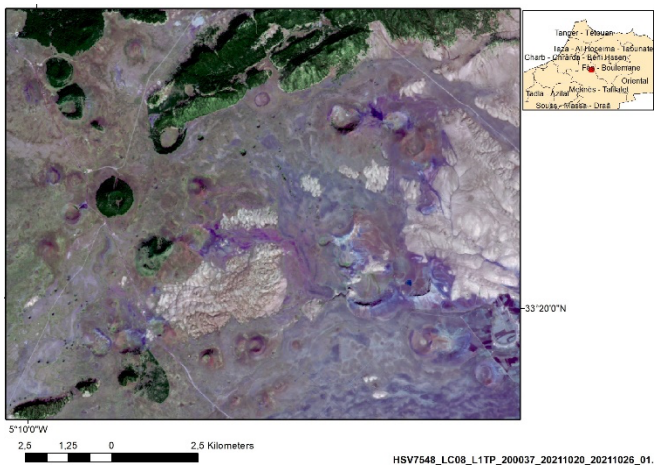


Fig. 17. Limestones and dolomites in contact with lava sheets within the Azrou-Timahdite plateau visible on a Landsat 8-scene HSV, Bands 2,7, 10 and 8).

The next example comprises both, a larger, circular basin with smaller ring structures. Fig. 18a, 18b, and 18c present the Oulmes volcanic area on a slope gradient map, drop raster scene, radar image and a Landsat scene. The Oulmes volcanic area (5°45′W to 6°00′W, 33°10′N to 33°20′N) forms a complex circular crater basin of a about 20 km in diameter with intrusions of smaller magmatic bodies. Cinder cones up to 2 km in diameter were mapped as black dots in Fig. 19c. The alkaline volcanic field was active during the Pliocene and Pleistocene [28]. A large fault zone striking WSW-ENE is visible at the southern border. A circular structure appears on the slope gradient map of the area around the city of El Menzel (4°40′W to 4°25′W and33°45′N to 33°55′N) with a diameter

*European Journal of Environment and Earth Sciences*
*www.ej-geo.org*

of about 6 km. From the slope gradient map based on ALOS PALSAR DEM datathe lowest slope degrees were extracted and presented in dark-green colors (Fig. 19). Along the concentrically arranged hills surrounding this enclosed topographic depression caves and springs in the Jurassic outcrops are documented [4]. Slope failure directed towards the depression center can be detected on Google Earth images.

The cause of the circular outline of the depression and its surrounding hills is still unknown and in the discussion. Another example of smaller ring structures related to karst features developed in the Jurassic and Cretaceous series is presented from the west coast of Morocco. Almost flat-floored solution sinkholes occur mainly at height levels from 30 up to 130 m and in flat areas with slope degrees <10°; see Fig. 20a and 20b. Their rim sides range from gently sloping to vertical, and their overall form can range from bowl-shaped to sometimes conical or even cylindrical floods produce rapid changes in the karstification processes [32], [33].

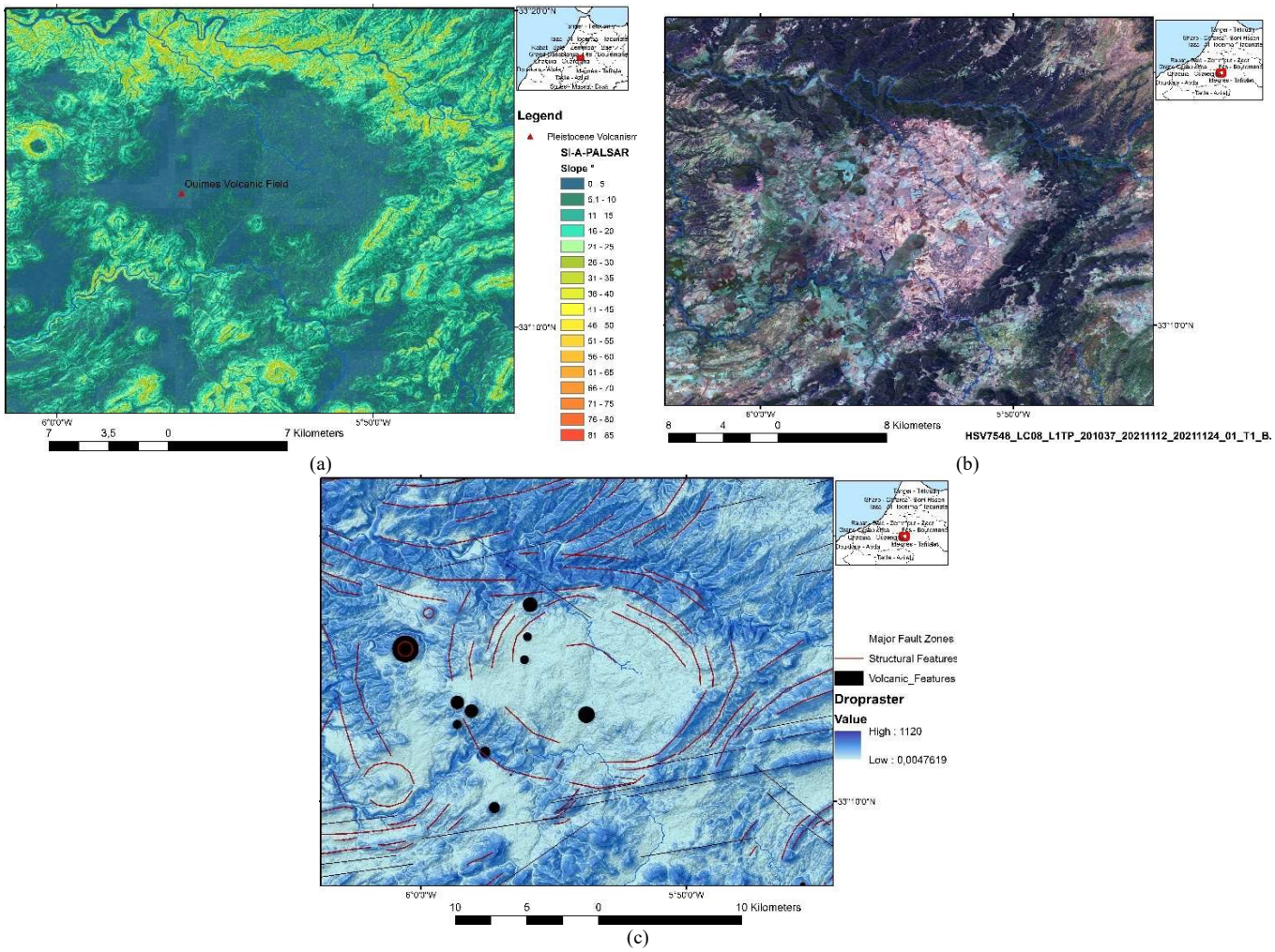


18. a) Slope gradient map of the Quaternary Oulmes volcanic field (39 on Fig. 1); b) Landsat 8-scene of the Oulmes volcanic area; c) Drop raster map based on ALOS-PALSAR-DEM data and structural evaluation. (The drop raster is calculated as the difference in z- value divided by the path length between the cell centers, expressed in percentages. For adjacent cells, this is analogous to the percent slope between cells. Across a flat area, the distance becomes the distance to the nearest cell of lower elevation. The result is a map of percent rise in the path of steepest descent from each cell. - ArcGIS Help).

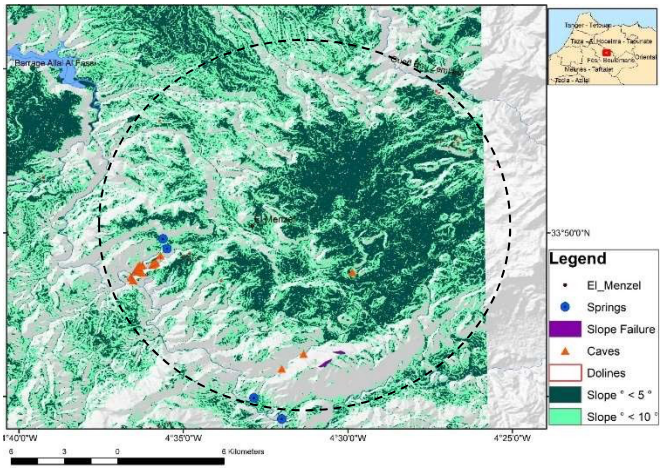


Fig.19. Slope gradients < 10 ° extracted from ALOS-PALSAR DEM data enhancing the circular outline of the depression around the city of El Menzel.

The structural evaluation reveals the close relationship of the sinkholes with the position and orientation of larger fault zones, mainly those striking SW-NE. There are regional differences in the karst doline patterns, most of them following tectonic structures such as fault and fracture zones. Larger sinkholes (about 100 m in diameter) can be identified on the satellite images. Ring structures are the result of cosmic impacts as well. Smaller, most bowl-shaped impact craters were identified in NW-Africa (Fig. 21). Although only one impact crater was documented so far in Morocco in the Earth Impact Data base [36], it can be assumed that more will be verified in the future with ongoing research.

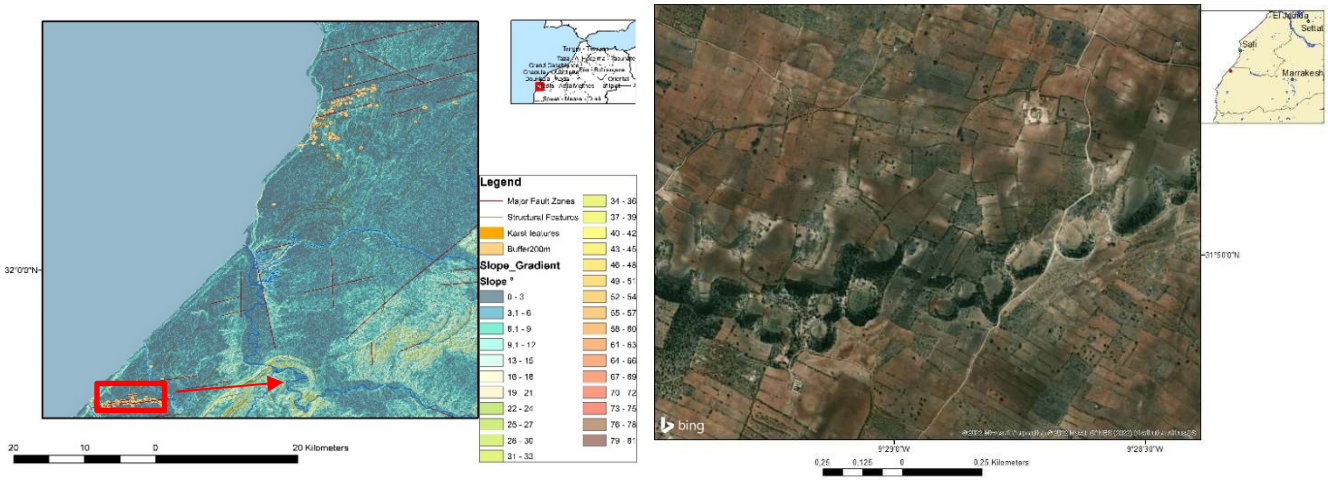


(a) (b)

Fig. 20. a) Slope gradient map based on ALOS PALSAR DEM data enhancing the visibility of larger fault zones influencing the occurrence of sinkholes; b) Uvala karst system following in its distribution larger fault zones visible on high resolution images from BingMap / Microsoft.

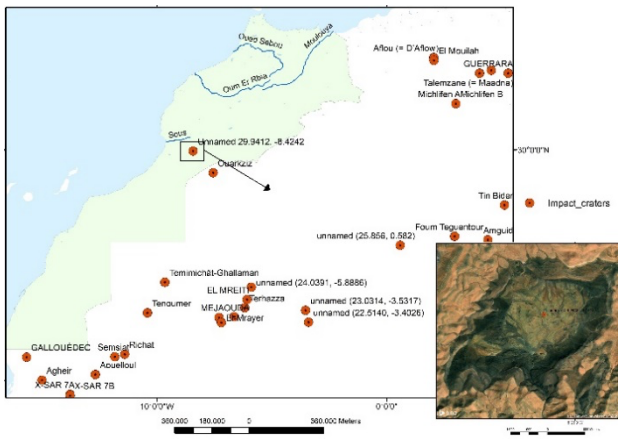


Fig. 21. Documented impact craters in NW-Africa [36].

## VI. Conclusion

The inventory of circular structures in Morocco is an important task, not only for geoscientific and economic reasons such as mineral exploration, but also as part of a georisk assessment to contribute to the safety of the land use and infrastructure. For example: The collapse of sinkholes might cause severe damage, as well as volcanic activity.

The evaluations of different satellite data lead to a more detailed inventory of ring structures of various sizes and origins in N- and NW-Morocco and to the detection of some circular structures, sometimes buried underneath younger sediments, mainly traced by the concentric arrangement of the drainage and vegetation pattern. The GIS embedded evaluation of morphometric maps, digital processed and enhanced optical satellite data and radar images allows the detection of even partly unknown structural features.

The geologic origin of these structures is complex and different, sometimes interacting with each other such as in the case of sinkhole developments near volcanic fields. The larger ring structures are mostly related to plutons, but also to salt domes due to salt diapirism along the coastal areas [34].

The evaluation feasibilities of satellite data come to limits when the origin of circular features cannot be identified.

The systematic, GIS integrated inventory of ring structures should be divided according to their origin. For example:

- a GIS related to large magmatic bodies,
- a GIS gathering information related to volcanicfeatures,
- a GIS containing karst information,
- a GIS related to salt tectonics.

Geohazards can be single, sequential, or combined in their origin and effects [35]. Thus, in the final step all the informationshould be summarized into a natural hazard GIS of Morocco to improve the georisk assessment and monitoring within a multi-hazard risk framework.

## Acknowledgment

The author thanks the reviewers and the EJGEO-Team for all their efforts. Mr. Iliass Nouadir, Laboratory of Geosciences, Environment and Associated Resources. Geology Department. Faculty of Sciences Dhar El Mahraz. Sidi Mohamed Ben Abdellah University, Fez, is kindly acknowledged for his contribution to discussions and for providing material.

## Funding

This study was funded by own resources.

## Conflict of Interest

The author declares that she does not have any conflict of interest.

## REFERENCES

[1] Michard A, Saddiqi O, Chalouan A, Frizon de Lamott D (Eds.): Continental Evolution: The Geology of Morocco, Structure, Stratigraphy, and Tectonics of the Africa-Atlantic-Mediterranean Triple Junction. Springer Berlin Heidelberg, 2008; Lecture Notes 133 in Earth Sciences 116, ISSN: 0930-0317.

[2] Tawadros E. Geology of North Africa. CRC Press, Taylor & Francis Group, a Balkema book, Version Date: 2011-12-07, International Standard Book Number-13, 978-0-415-89146-2.

[3] Ennih N, Liégeois JP. The boundaries of the West African craton, with special reference to the basement of the Moroccan metacratonic Anti-Atlas belt. *Geological Society*, London, Special Publications, 2008; 297: 1-17. doi:10.1144/SP297.1.

[4] Theilen-Willige B, Naouadir I. Contribution of Remote Sensing and GIS to the Inventory and Analysis of Factors influencing the Development of Karst Features in the Middle Atlas, Morocco. *European Journal of Environment and Earth Sciences*, Nov. 2022;3 (6): 1-17. DOI: http://dx.doi.org/10.24018/ejgeo.2022.3.6.330.

[5] European-Mediterranean Seismological Centre (EMSC) Available from: https://www.emsc-csem.org/Earthquake/?filter=yes.

[6] International Seismologica] Centre (ISC), Available: http://www.isc.ac.uk/iscbulletin/search/catalogue/interactive/

[7] US Geological Survey (USGS). Available from: https://earthquake.usgs.gov/earthquakes/search/

[8] OneGeology portal, British Geological Survey. Availabe from: http://portal.onegeology.org/OnegeologyGlobal/, Geology of Morocco at 1:5 million scale. 2019. https://map.bgs.ac.uk/arcgis/services/AGA/BGS_Groundwater/MapServer/WmsServer?

[9] Geologic Shapefiles. Available from: http://www.mediafire.com/file/7vhwkevolkm94bl/g%C3%A9ologie+maroc.zip.

[10] Hafid M, Zizi M, Bally AW, Ait Salem A. Structural styles of the western onshore and offshore termination of the High Atlas, Morocco. *Comptes Rendus Geoscience*, January 2006; 338(1–2): 50-64. https://doi.org/10.1016/j.crte.2005.10.007.

[11] Yaaqoub A, Essaïfi A, Clementucci R, Ballato P, Faccenna C. Late Cenozoic tectonic deformation and mantle-driven uplift in the Middle Atlas mountain belt (Morocco). EGU General Assembly, 2021; EGU21-13646. Available from: https://www.google.de/url?sa=t&rct=j&q=&esrc=s&source=web&cd=&ved=2ahUKEwiTt4LX_M77AhUiYPEDHZQ_CKw4ChAWegQIChAB&url=https%3A%2F%2Fpresentations.copernicus.org%2FEGU21%2FEGU2113646_presentation.pdf&usg=AOvVaw0gRSNkIMLKcITWm415EU.

[12] Mounir S, Saoud N, Charroud M, Mounir, K, Choukrad J. The Middle Atlas Geological karsts forms: Towards Geosites characterization. *Oil & Gas Science and Technology* - Revue de l IFP. 2019;74(3–5). DOI:10.2516/ogst/2018089.

[13] Frizon de Lamotte D, Zizi M, Missenard Y, Hafid M, El Azzouzi M, Maury RC, Charriere A, Taki Z, M. Benammi M, Michard A. The Atlas System. In: Michard A, Saddiqi O, Chalouan A, Frizon de Lamotte D (Eds.): Continental Evolution: The Geology of Morocco, Structure, Stratigraphy, and Tectonics of the Africa-Atlantic-Mediterranean Triple Junction. Springer Berlin Heidelberg, 2008, Chapter 4, Lecture Notes in Earth Sciences 116: 133-202, ISSN: 0930-0317.

[14] Soulaimani A, Michard A, Ouanaimi H, Baidder L, Raddi Y, Saddiqi O, Rjimati EC. Late Ediacaran–Cambrian structures and their reactivation during the Variscan and Alpine cycles in the Anti-Atlas (Morocco). *Journal of African Earth Sciences*, Oct. 2014; 98: 94-112. https://doi.org/10.1016/j.jafrearsci.2014.04.025.

[15] Marzoli A, Bertrand H, Youbi N, Callegaro S, Merle R, Reisberg L, Chiaradia M, *et al.* The Central Atlantic Magmatic Province (CAMP) in Morocco. *Journal of Petrology*, 2019; 60(5): 945–996. https://doi.org/10.1093/petrology/egz021.

[16] Ikenne M, Souhassou M, Arai S, Soulaimani A. A historical overview of Moroccan magmatic events along northwest edge of the West African Craton. *Journal of African Earth Sciences*. March 2017; 127: 3-15. https://doi.org/10.1016/j.jafrearsci.2016.10.002.

[17] Marzoli A, Bertrand H, Youbi N, Callegaro S, Merle R, *et al.* The Central Atlantic Magmatic Province (CAMP) in Morocco. *Journal of Petrology*. 2019; 60(5): 945–996. doi: 10.1093/petrology/egz021.

[18] Tari G, Haddou Jabour H. Salt Tectonics in the Atlantic Margin of Morocco. *Search and Discovery Article #30061*. Posted October 30, 2008; Adapted from oral presentation at AAPG Annual Convention, San Antonio, Texas, April 20-23, 2008. http://www.searchanddiscovery.com/documents/2008/08192tari/images/tari.pdf.

[19] Tari G, Novotny B, Jabour H, Hafid M. Salt Tectonics Along the Atlantic Margin of NW Africa (Morocco and Mauritania). *Permo-Triassic Salt Provinces of Europe, North Africa and the Atlantic Margins*, 2017: 331–351. https://doi.org/10.1016/b978-0-12-809417-4.00016-1.

[20] Thiéblemont D. Geological Map of Africa at 1:10 Mscale, CGMW-BRGM, 2016. ISBN: 9782917310328. doi: 10.14682/2016GEOAFR.

[21] Hollard H, Choubert G, Bronner G, Marchand J, Sougy J, *et al.* Carte Géologique du Maroc, scale 1: 1.000.000 - Serv. Carte géol. Maroc, 1985.

[22] USGS EarthExplorer. Available: https://earthexplorer.usgs.gov/.

[23] European Space Agency (ESA), Copernicus Open Access Hub. Available from: https://scihub.copernicus.eu/dhus/#/home.

[24] Geofabrik's free download server. Available from: http://download.geofabrik.de/africa.html.

[25] Alaska Satellite Facility (ASF) Data Search Vertex. *NASA Earth Data*. Available from: https://search.asf.alaska.edu/#/

[26] TanDEM-X - Digital Elevation Model (DEM) - Global, 90m. Available from: https://download.geoservice.dlr.de/TDM90/.

[27] Theilen-Willige B. Geomorphologic and geologic Analysis of Satellite Data of the Betic and Rif orogenic Belts in the Western Mediterranean Sea. *European Journal of Environment and EarthSciences*. April 2022; 3(2): 73-79. DOI: http://dx.doi.org/10.24018/ejgeo.2022.3.2.276.

[28] Mountaj S, Remmal T, Lakroud K, Boivin P, El Hassani el Amrani I, El Kamel F, Makhoukhi S, *et al.* The Volcanic Field of the Middle Atlas Causse: Highlights and Heritage Appropriation. *The Geographical Bulletin,* 60(2): 127-147.

[29] Melis MT, Pisani L, De Waele J. On the Use of Tri-Stereo Pleiades Images for the Morphometric Measurement of Dolines in the Basaltic Plateau of Azrou (Middle Atlas, Morocco. *Remote Sens*. 2021; 13, 4087. https://doi.org/10.3390/rs13204087.

[30] Mhiyaoui H, Ahmed Manar A, Remmal T, Boujamaoui M, El Kamel F, Amar M, Mansour M, El Hassani El Amrani I. Structures profondes du volcanisme quaternaire du Moyen Atlas central (Maroc): Apports de la cartographie aéromagnétique - Deep quaternary volcanic structures in the central Middle Atlas (Morocco): Contributions of aeromagnetic mapping. *Bulletin de l'Institut Scientifique*, Rabat, Section Sciences de la Terre. 2016; 38: 111-125. e-ISSN: 2458-7184.

[31] Amine A, El Hassani El Amrani I, Remmal T, El Kamel F, Van wyk de Vries B, Boivin P. Geomorphological Classification and Landforms Inventory of the Middle-Atlas Volcanic Province (Morocco): Scientific Value and Educational Potential. *Quaestiones Geographicae*. March 2019; 38(1). DOI: 10.2478/quageo-2019-0010.

[32] Habiballah R, Witam O, Ibnoussina M. Relationship between Karstification and Tectonism in the Upper Jurassic Evaporite Formation: A Case Study of the Lalla Fatna Escarpment Safi, Morocco. *Iraqi Geological Journal*. 2022; 55(2D): 54-63. DOI: 10.46717/igj.55.2D.5ms-2022-10-21.

[33] Theilen-Willige B, Ait Malek H, Charif A, El Bchari F, Chaïbi M. Remote Sensing and GIS Contribution to the Investigation of Karst Landscapes in NW-Morocco. *Geosciences*, 2014; 4(2): 50-72. https://doi.org/10.3390/geosciences4020050.

[34] Davison I, Anderson LM, Bilbo, M. Salt Tectonics and Sub-salt Exploration Plays in the Essaouira Basin, Morocco. *II Central & North Atlantic Conjugate Margins Conference, Rediscovering the Atlantic, New winds for an old sea*. 2010; VI: 76-78. http://metododirecto.pt/CM2010. ISBN: 978-989-96923-1-2.

[35] Van Westen C, Michiel Damen M, Feringa W. National Scale Multi-Hazard Risk Assessment, Training Package on National Scale Multi-Hazard Risk Assessment, Theory Book PPRD-EAST. University Twente, Faculty of Geo-Information Science and Earth Observation (ITC), 2013: 175. Available from: https://www.academia.edu/30308280/Training_Package_on_National_Scale_Multi_Hazard_Risk_Assessment_National_Scale_Multi_Hazard_Risk_Assessment_Theory_Book?email_work_card=view-paper.

[36] Earth Impact Database–Africa. The Planetary and Space Science Centre (PASSC), Canada. Available: http://www.passc.net/EarthImpactDatabase/New%20website_052018/Africa.html.

*European Journal of Environment and Earth Sciences*
*www.ej-geo.org*

**Prof. Dr. Barbara Theilen-Willige** (retired) worked at the Institute of Applied Geosciences, Faculty VI, Technische Universität Berlin (TUB), Berlin, Germany. From 2018 until 2020 she lectured in the Central Department El Gouna of TUB, Department of Water Engineering in El Gouna, Egypt. She was involved as well in lecturing activities at universities in Yogyakarta and Semarang, Java, Indonesia for the Senior Expert Service (SES), Bonn. Prof. Barbara Theilen-Willige does research in the fields of geomorphology, geology, remote sensing and GIS-methods.
https://orcid.org/0000-0002-9206-7362
https://www.researchgate.net/profile/Barbara-Theilen-Willige